Title

Mechanochemical Synthesis, Accelerated Aging, and Thermodynamic Stability of the Organic Mineral Paceite and Its Cadmium Analogue

Journal

ACS Omega, 4(3)

ISSN

2470-1343

Authors

Li, Shaodi
Huskić, Igor
Novendra, Novendra
et al.

Publication Date

2019-03-31

DOI

10.1021/acsomega.9b00295

Peer reviewed

ACS OMEGA

Article

Cite This: ACS Omega 2019, 4, 5486−5495

http://pubs.acs.org/journal/acsodf

Mechanochemical Synthesis, Accelerated Aging, and Thermodynamic Stability of the Organic Mineral Paceite and Its Cadmium Analogue

Shaodi Li,[‡,†] Igor Huskić,[‡,†] Novendra Novendra,[§] Hatem M. Titi,[‡] Alexandra Navrotsky,*[,§] and Tomislav Friščić*[,‡]

[‡]Department of Chemistry, McGill University, 801 Sherbrooke St. W., H3A 0B8 Montreal, Canada

[§]Peter A. Rock Thermochemistry Laboratory and NEAT ORU, University of California Davis, One Shields Avenue, Davis, California 95616, United States

Supporting Information

ABSTRACT: We demonstrate the use of ball milling mechanochemistry for rapid, simple, and materials-efficient synthesis of the organic mineral paceite $CaCu(OAc)_4{\cdot}6H_2O$ (where OAc^- is the acetate ion), composed of coordination polymer chains containing alternating Ca^{2+} and Cu^{2+} ions, as well as its cadmium-based analogue $CaCd(OAc)_4{\cdot}6H_2O$. While the synthesis of paceite in aqueous solutions requires a high excess of the copper precursor, mechanochemistry permits the use of stoichiometric amounts of reagents, as well as the use of poorly soluble and readily accessible calcium carbonate or hydroxide reactants. As established by thermochemical measurements, enthalpies of formation of both synthetic paceite and its cadmium analogue relevant to the mechanochemical reactions are highly exothermic. Reactions can also be conducted using accelerated aging, a synthetic technique that mimics geological processes of mineral weathering. Accelerated aging reactivity involving copper(II) acetate monohydrate (hoganite) and calcium carbonate (calcite) provides a potential explanation of how complex organic minerals like paceite could form in a geological environment.

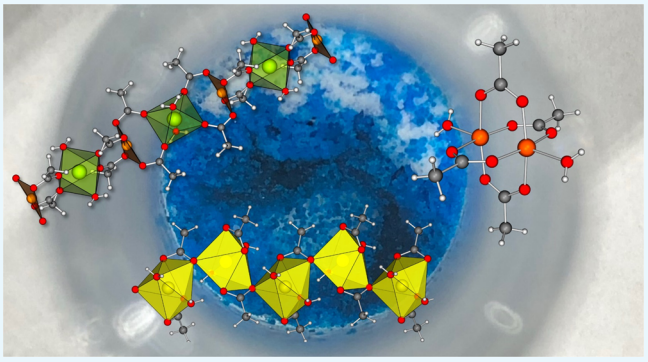

INTRODUCTION

Over the past 10 years, structural studies of geological samples have identified an increasing number of organic minerals, broadly defined as carbon-bearing mineral species other than carbonates and carbon allotropes.[1,2] Principal representatives of such organic minerals are transition metal and lanthanide oxalates,[3,4] as well as metal formates,[5] mellitates,[6] acetates,[1,2] and organic molecules such as uric acid.[7−9] The search for organic minerals and a deeper understanding of their structures and origins have been additionally promoted by the recent "Carbon Mineral Challenge" initiative, which considers organic minerals, while extremely poorly investigated, as nevertheless central to understanding mineral evolution and carbon cycle on Earth and other planetary systems.[10,11] The vibrant investigations of organic minerals have recently led to the structural characterization of geoporphyrins,[12] discovery of naturally occurring metal−organic frameworks (MOFs),[13,14] and proposed geological appearance of organic cocrystals[15] in extraterrestrial environments such as Titan.[16]

Recent additions to the library of organic minerals are copper(II) acetate monohydrate, $Cu(OAc)_2{\cdot}H_2O$, found as the mineral hoganite in the Potosi Mine in New South Wales (Australia), and paceite, the related double salt of calcium copper(II) acetate hexahydrate, $CaCu(OAc)_4{\cdot}6H_2O$, found as dark blue crystals growing on the surface of hoganite specimens.[17] The minerals found in gossan were goethite, hematite, quartz, linarite, malachite, azurite, cuprian smithsonite, and cerussite. Gossan was located at a depth of approximately 20 m and in the vicinity of a decomposing leaf litter, providing a potential source of acetate ion. The structures of both minerals are unique in the context of organic minerals, representing the first identified acetate minerals,[17] and are also of relevance to modern metal−organic materials chemistry. In particular, hoganite consists of the well-known copper(II) acetate "paddlewheel" dimers (Figure 1), which are also important secondary building units in the design and synthesis of coordination polymers and metal−organic frameworks (MOFs).[18] Calcium copper(II) acetate hexahydrate is a synthetic compound that has been known since at least 1960,[19] and its single crystal X-ray diffraction structure was reported first by Langs and Hare in 1967,[20] who described the structure without detailed crystallographic data. The structure was

Received: February 1, 2019
Accepted: March 5, 2019
Published: March 19, 2019

DOI: 10.1021/acsomega.9b00295
ACS Omega 2019, 4, 5486−5495

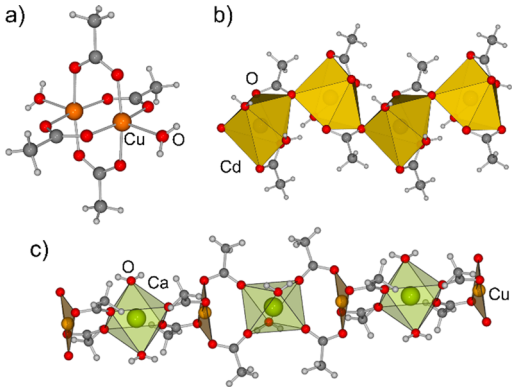

Figure 1. (a) Structure of the paddlewheel unit found in the crystal structure of $Cu(OAc)_2{\cdot}H_2O$ (hoganite mineral) and (b) fragment of the crystal structure of $Cd(OAc)_2{\cdot}2H_2O$, with coordination environments around cadmium ions shown as yellow polyhedra. (c) Fragment of a single bimetallic coordination polymer chain in the crystal structure of paceite, $CaCd(OAc)_4{\cdot}6H_2O$, with calcium and cadmium ion coordination environments shown as green and yellow polyhedra, respectively.

subsequently redetermined by Klop et al.[21] and by El-Bali and Bolte[22] and consists of one-dimensional coordination polymer chains of alternating square-coordinated copper(II) ions and hydrated octahedrally coordinated calcium ions bridged by acetate ions. Such regular alternation of metal ions is also of relevance for the development of metal−organic materials based on more than one type of metal ion. In particular, while a number of designs have recently emerged for such mixed-metal materials,[23,24] these are usually based on the formation of solid solutions in which different metal ions are randomly distributed over specific crystallographic sites.[25] The potentially broader relevance of this structure in metal−organic chemistry is highlighted by its cadmium- and calcium-based analogue, $CaCd(OAc)_4{\cdot}6H_2O$. This compound was described by Balarew and Stoilova,[26] as well as by Langs and Hare, who also conducted structural characterization.[20] The compound was reported to be isomorphous to $CaCu(OAc)_4{\cdot}6H_2O$, but detailed crystallographic information was never provided.

Consequently, we recognized paceite and its synthetic cadmium analogues as excellent targets for our ongoing investigation of the properties and potential origin of naturally occurring metal−organic materials.[13,27] Specifically, we targeted the structure, thermal, and thermodynamic stability of synthetic paceite and its cadmium analogue, as well as potential routes through which such materials could assemble from geologically relevant precursors, via mechanochemical[28] or accelerated aging[29] reactions.

EXPERIMENTAL SECTION

Mechanochemical syntheses were conducted using either a Retsch MM200 mixer mill operating at 25 Hz or a Form-Tech Scientific 1000 shaker mill operating at 30 Hz. All reactions were performed using stainless steel milling media, including a milling jar of 15 mL volume equipped with two milling balls of 7 mm diameter (1.37 g each). A detailed mechanochemical reaction procedure for each compound is given in the Supporting Information.

Differential scanning calorimetry coupled with thermogravimetric analysis (DSC-TG) was performed on a Netzsch 449 instrument to determine the water content of the samples. In each experiment, the samples were heated from 25 to 800 °C under an O_2 atmosphere (heating rate 10 °C/min, platinum crucible).

Fourier transform infrared attenuated total reflectance (FTIR-ATR) spectra were obtained using a Bruker Platinum ATR spectrometer.

In situ PXRD monitoring of aging reactions was performed on a PROTO AXRD Benchtop diffractometer equipped with a DECTRIS Mythen 1K strip detector. Data were collected using a custom designed sample holder.[30] A homogenized mixture of $Ca(OH)_2$ and $Cu(OAc)_2{\cdot}H_2O$ was placed in the middle, and 200 mL of 50% aqueous solution (by volume) of acetic acid was placed in the sample holder grooves. Consecutive powder diffractograms were collected over the course of 12 h with a time resolution of 5 min and 50 s between scans. Rietveld fitting was performed in the TOPAZ6 analytical program.[31]

Single crystal X-ray diffraction data were collected on a Bruker D8 Advance diffractometer with a Photon 200 CMOS area detector and an IμS microfocus X-ray source (Madison, WI) using Mo Kα radiation. The single crystal was coated with paraffin oil, and data were collected at room temperature. The Apex3 software suite (Madison, WI) was used for data collection, reduction, and unit cell assignment.

The enthalpy of dissolution of the samples was measured using a CSC (Calorimetry Sciences Corporation) 4400 isothermal microcalorimeter at 25 °C. In each experiment, 5−15 mg of the sample was hand-pressed to form a pellet and dropped into a Teflon cell in the calorimeter filled with 25 g of 5 N HCl solvent. All weight measurements were done using a Mettler microbalance with an accuracy of 10 μg. The solvent was isothermally equilibrated for at least 3 h under mechanical stirring before the introduction of the sample, and the sample was allowed to dissolve in the cell for at least 3 h, ensuring the return of baseline back to the initial position. For each experiment, the solvent in the cell was replaced with a new fresh solvent. The collected data were integrated with a baseline correction and converted to joules using a calibration factor to obtain the total heat effect due to the dissolution of the sample. To obtain the calibration factor, the NIST standard reference material KCl was used. The calibration was done by dissolving 15 mg of KCl pellet into 25 g of H_2O, which corresponds to a reference concentration of 0.008 mol/kg at 25 °C. The calibration factor was obtained by correlating the integrated data with a known enthalpy of dissolution and dilution of 0.008 mol/kg KCl. For each sample, at least four measurements were performed, and their average was reported as the final value. The uncertainties given in the result represent 95% confidence interval. This experimental method is the same as the one used in our earlier study of metal−organic frameworks.[32]

RESULTS AND DISCUSSION

Mechanochemical Synthesis of Synthetic Paceite and Its Cadmium Analogue. Synthesis of artificial paceite from water was described in 1960 by Holden and Singer using copper(II) acetate monohydrate and calcium acetate as starting materials.[19] The synthesis is a textbook example of noncongruent cocrystallization, as the aqueous solubility of calcium acetate is significantly higher than that of $Cu(OAc)_2{\cdot}H_2O$, which requires the two components to be used in a non-stoichiometric approximately 4:1 ratio. Mechanochemistry by ball milling has been demonstrated to

DOI: 10.1021/acsomega.9b00295
ACS Omega 2019, 4, 5486−5495

provide access to solubility-independent reactions in which the stoichiometric composition of the product can be readily controlled by the composition of the reaction mixture.[33,34] Such stoichiometry control was observed for mechanochemistry by neat (dry) milling, as well as by liquid-assisted grinding (LAG), a methodology that uses a small amount of a liquid phase (measured in the form of η, the ratio of liquid additive to reactant weight) to enable and accelerate mechanochemical reactions.[32] Consequently, we decided to explore whether mechanochemistry can be used to obtain synthetic paceite samples using stoichiometric amounts of Cu^{2+} and Ca^{2+} precursors.

For that purpose and with the intention to explore potential routes through which paceite could be formed in a geological environment, we envisaged a two-step synthetic protocol that would use mineral-like substances as precursors. We chose copper(II) acetate monohydrate, $Cu(OAc)_2{\cdot}H_2O$, as a source of Cu^{2+} ions, while the calcium acetate material required for the synthesis would be obtained in a mechanochemical reaction of either $CaCO_3$ or $Ca(OH)_2$ in combination with acetic acid (AcOH) (reactions 1 and 2). The resulting hydrated calcium acetate was then expected to form paceite in a mechanochemical reaction with 1 equiv of $Cu(OAc)_2{\cdot}H_2O$ (reaction 3).

$$CaCO_{3(s)} + 2AcOH_{(l)} \rightarrow Ca(OAc)_2{\cdot}H_2O_{(s)} + CO_{2(g)} \quad (1)$$

$$Ca(OH)_{2(s)} + 2AcOH_{(l)} \rightarrow Ca(OAc)_2{\cdot}H_2O_{(s)} + H_2O_{(g)} \quad (2)$$

$$Ca(OAc)_2{\cdot}H_2O_{(s)} + Cu(OAc)_2{\cdot}H_2O_{(s)} + 4H_2O_{(l)} \rightarrow CaCu(OAc)_4{\cdot}6H_2O_{(s)} \quad (3)$$

All mechanochemical reactions were performed by the LAG methodology[35] using a small amount of water as an additive (typically 10−12 μL, see the Supporting Information), and analysis of reactants by PXRD confirmed that the used $CaCO_3$ was in the calcite form. The LAG reactions of either $Ca(OH)_2$ or $CaCO_3$ with a small excess (under 5 mol %) of glacial acetic acid led to the formation of calcium acetate monohydrate as the sole crystalline product. In particular, milling 0.5 mmol of $Ca(OH)_2$ for 30 min with 60 μL of AcOH and 10 μL of water led to the complete disappearance of the solid reactant and formation of hydrated calcium acetate of the formula $Ca(OAc)_2{\cdot}H_2O$ (CSD code CEJLIM), identified by powder X-ray diffraction (PXRD) and thermogravimetric analysis (TGA) (Figure 2, also see the Supporting Information). In contrast, complete conversion of $CaCO_3$ into $Ca(OAc)_2{\cdot}H_2O$ required 80 min of milling on the 1 mmol scale (see the Supporting Information). Shorter milling times revealed the formation of a mixed hydrate and acetic acid solvate of calcium acetate, of composition $Ca(OAc)_2{\cdot}H_2O{\cdot}AcOH$, which was identified by PXRD reflections matching those simulated for the published structure (CSD code COKJUH), along with unreacted $CaCO_3$. Upon longer milling, the initially formed $Ca(OAc)_2{\cdot}H_2O{\cdot}AcOH$ reacted with remaining $CaCO_3$ to provide $Ca(OAc)_2{\cdot}H_2O$ (Figure 3).

In the next step, 1 equiv of $Cu(OAc)_2{\cdot}H_2O$ was added to the mechanochemically prepared $Ca(OAc)_2{\cdot}H_2O$ and the reaction mixture was milled for an additional 30 min. Analysis by PXRD revealed the complete disappearance of Bragg reflections of the starting materials and appearance of new reflections consistent with the diffraction pattern calculated for the crystal structure of paceite. Identical outcomes were obtained regardless of whether the Ca^{2+} source in this two-step process was calcium carbonate or hydroxide (Figure 2). The formation of the paceite structure was also possible in a one-pot one-step process by milling calcium carbonate or hydroxide and acetic

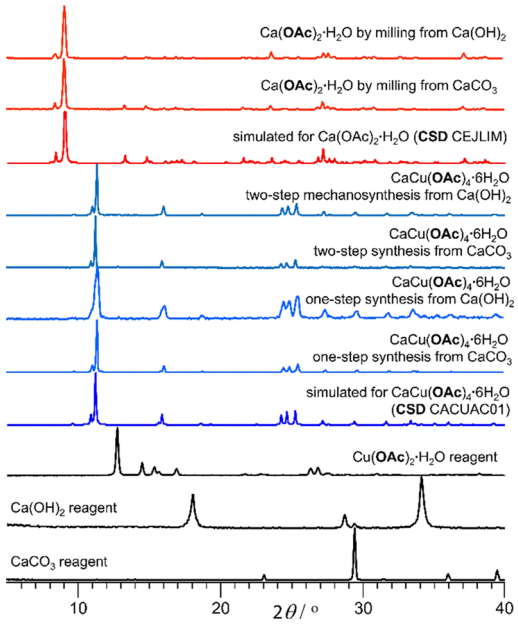

Figure 2. Comparison of PXRD patterns for $Ca(OAc)_2{\cdot}H_2O$ mechanochemically prepared from $Ca(OH)_2$ or $CaCO_3$ and for samples of $CaCu(OAc)_4{\cdot}6H_2O$ (synthetic paceite) prepared in a one- or two-step mechanochemical procedure to corresponding patterns of starting materials and simulated patterns of targeted products.

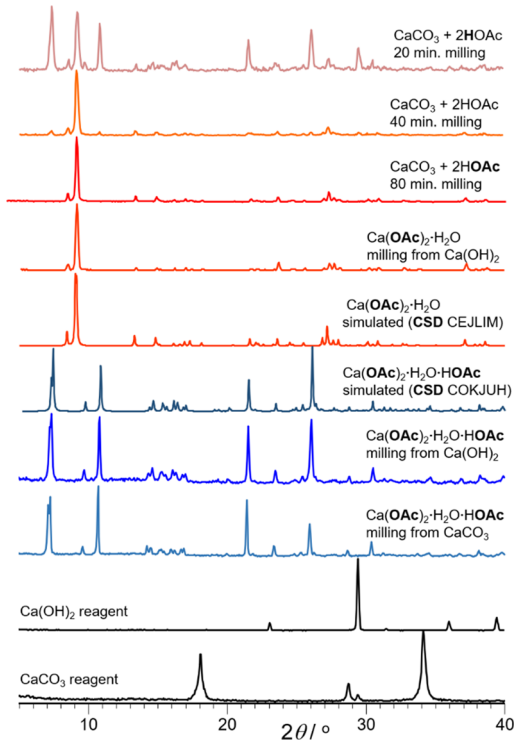

Figure 3. Overlay of PXRD patterns for $Ca(OAc)_2{\cdot}H_2O{\cdot}AcOH$ mechanochemically synthesized from $Ca(OH)_2$ or $CaCO_3$ to relevant patterns of reactants and simulated patterns.

DOI: 10.1021/acsomega.9b00295
ACS Omega 2019, 4, 5486−5495

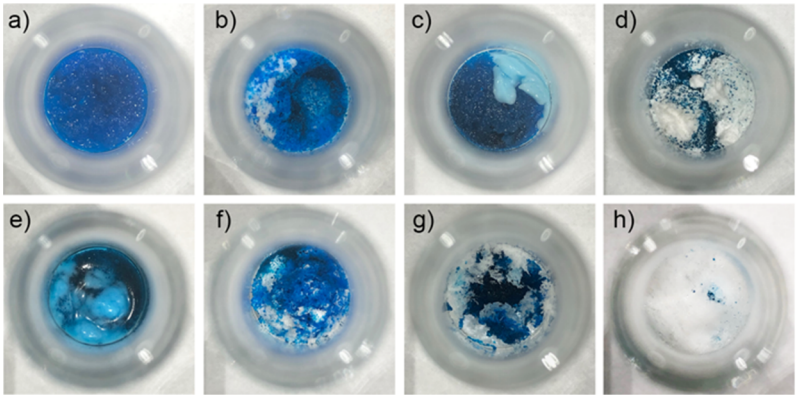

Figure 4. Optical images of equimolar mixtures of $Cu(OAc)_2{\cdot}H_2O$ and either $Ca(OH)_2$ or $CaCO_3$ upon 6 days of aging under different conditions: (a) $Cu(OAc)_2{\cdot}H_2O$ and $Ca(OH)_2$ with 1.1 equiv of AcOH added directly to the mixture and aged at 100% RH and 45 °C; (b) $Cu(OAc)_2{\cdot}H_2O$ and $Ca(OH)_2$ with 1.1 equiv of AcOH added directly to the mixture and aged at 100% RH and room temperature; (c) $Cu(OAc)_2{\cdot}H_2O$ and $Ca(OH)_2$ aged in vapors of 50% aqueous AcOH at 45 °C; (d) $Cu(OAc)_2{\cdot}H_2O$ and $Ca(OH)_2$ aged in vapors of 50% aqueous AcOH at room temperature; (e) $Cu(OAc)_2{\cdot}H_2O$ and $CaCO_3$ with 1.1 equiv of AcOH added directly to the mixture and aged at 100% RH and 45 °C; (f) $Cu(OAc)_2{\cdot}H_2O$ and $CaCO_3$ with 1.1 equiv of AcOH added directly to the mixture and aged at 100% RH and room temperature; (g) $Cu(OAc)_2{\cdot}H_2O$ and $CaCO_3$ aged in vapors of 50% aqueous AcOH at 45 °C; (h) $Cu(OAc)_2{\cdot}H_2O$ and $CaCO_3$ aged in vapors of 50% aqueous AcOH at room temperature.

acid in the presence of equimolar amounts of $Cu(OAc)_2{\cdot}H_2O$ and water. After 30 min of milling, the PXRD pattern of the reaction mixture exhibited only X-ray reflections of the mixed coordination polymer $CuCa(OAc)_4{\cdot}6H_2O$ (Figure 2). The formation of paceite by both one- and two-step mechanochemical routes was also confirmed by Fourier transform infrared attenuated total reflectance (FTIR-ATR) spectra, which were identical for the products of both synthetic methods (see the Supporting Information).

The described two-step and one-step mechanochemical routes to $CuCa(OAc)_4{\cdot}6H_2O$ clearly demonstrate that the synthesis of this material can be readily performed through LAG using only stoichiometric amounts of metal precursors.

Stoichiometric Control in Mechanochemical Synthesis of Calcium Acetate Solvates. The observed formation of $Ca(OAc)_2{\cdot}H_2O{\cdot}AcOH$ as an intermediate in the mechanochemical synthesis of $Ca(OAc)_2{\cdot}H_2O$ from $CaCO_3$ is consistent with previously reported formation of highly solvated compounds as intermediates in mechanochemical synthesis of coordination compounds and MOFs.[36−38] It also suggests the possibility for selective synthesis of different solvates of calcium acetate, $Ca(OAc)_2{\cdot}H_2O$ or $Ca(OAc)_2{\cdot}H_2O{\cdot}AcOH$, depending on the stoichiometric composition of the reaction mixture. Specifically, we speculated that simply using the calcium-based precursor and acetic acid in the respective stoichiometric ratio of 1:3 should enable the selective formation of $Ca(OAc)_2{\cdot}H_2O{\cdot}AcOH$. Indeed, milling of 1 mmol of $Ca(OH)_2$ with 3 mmol of AcOH led to the complete disappearance of Bragg reflections of the solid reactant in the PXRD pattern of the reaction mixture and the appearance of reflections of $Ca(OAc)_2{\cdot}H_2O{\cdot}AcOH$ (Figure 3). The formation of $Ca(OAc)_2{\cdot}H_2O{\cdot}AcOH$ was also verified by TGA. Similarly, milling of $CaCO_3$ with 3 equiv of AcOH led to quantitative conversion within 60 min of milling. Energetic constraints on these reactions and observed intermediates are discussed below from the point of view of thermochemical data.

The demonstrated ability to selectively obtain either $Ca(OAc)_2{\cdot}H_2O{\cdot}AcOH$ or $Ca(OAc)_2{\cdot}H_2O$ provides an additional illustration of the effectiveness of mechanochemical methods in controlling the stoichiometric composition of products.

Formation of Paceite by Accelerated Aging: A Potential Route for Geochemical Synthesis. The formation of paceite by two-step or one-step milling reaction of $CaCO_3$ and $Cu(OAc)_2{\cdot}H_2O$, both of which are known mineral species, suggests a possible geochemical route to paceite either through mechanical impact[39] or through mineral weathering reactions. In order to explore this possibility, we conducted accelerated aging reactions[40] inspired by mineral weathering processes[41] in which the exposure of inorganic minerals to small organic molecules under suitable conditions of temperature and atmosphere leads to the formation of organic minerals.

Two designs of accelerated aging reactions were explored. In one design, the reaction mixtures of either $Ca(OH)_2$ or $CaCO_3$ with 1 equiv of $Cu(OAc)_2{\cdot}H_2O$ were manually mixed, followed by addition of a slight excess (10 mol %) of liquid AcOH, and then left to age for 7 days in 100% relative humidity (100% RH, i.e., saturated water vapor). In the second reaction design, the mixtures of $Cu(OAc)_2{\cdot}2H_2O$ with either $CaCO_3$ or $Ca(OH)_2$ as the calcium source were left to age for 7 days in an atmosphere saturated by vapors of a 50% aqueous solution of acetic acid (v/v). The reactions were conducted either at room temperature or in an incubator set to 45 °C. Visual observation of reaction mixtures over time in most cases revealed partial deliquescence and change in reaction mixture color to blue, consistent with paceite formation (Figure 4). The exceptions were reactions in which mixtures of $Cu(OAc)_2{\cdot}H_2O$ with $CaCO_3$ or $Ca(OH)_2$ were left to age in vapors of the 50% aqueous acetic acid solution. Even after 7 days, these mixtures clearly consisted of a white powder with dispersed dark green particles of the $Cu(OAc)_2{\cdot}H_2O$ reactant.

The visual observations are confirmed by PXRD analysis of the aged reaction mixtures (Figure 5), which were briefly manually ground before recording a diffractogram. The analysis revealed the formation of the paceite structure in all experiments, except in the aforementioned reactions of aging in vapors of 50% aqueous AcOH solution (v/v) at room temperature. Importantly, while reaction mixtures exhibited

DOI: 10.1021/acsomega.9b00295
ACS Omega 2019, 4, 5486−5495

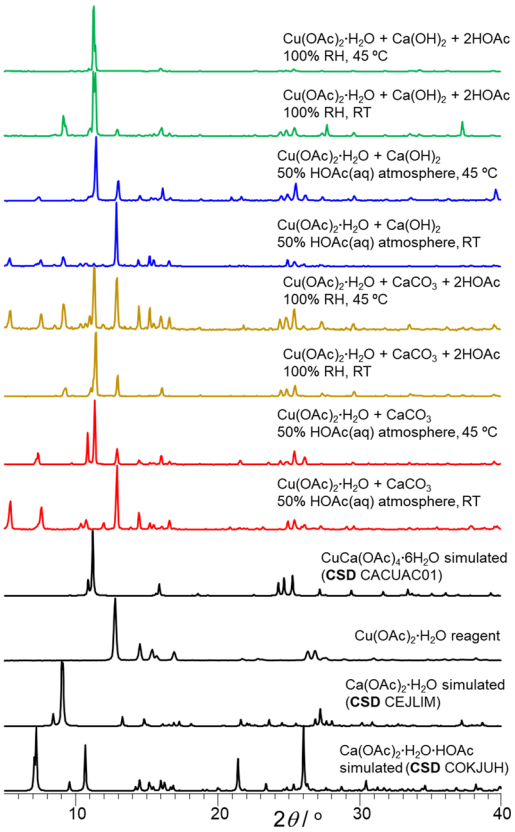

Figure 5. PXRD patterns for mixtures of $Cu(OAc)_2·H_2O$ with either $Ca(OH)_2$ or $CaCO_3$ after 7 days of aging under different conditions compared to simulated patterns of $CaCu(OAc)_4·6H_2O$, $Ca(OAc)_2·H_2O$, and $Ca(OAc)_2·H_2O·AcOH$. Reactions were kept either at 45 °C or at room temperature.

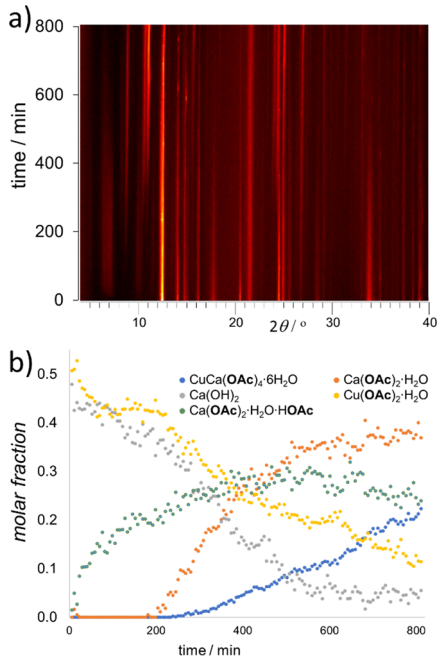

Figure 6. (a) Time-resolved X-ray powder diffractogram for the aging reaction of $Ca(OH)_2$ and $Cu(OAc)_2·H_2O$ in an atmosphere of water and acetic acid and (b) corresponding reaction profile based on Rietveld refinement of the PXRD data.

deliquescence, in no case was complete dissolution of samples observed.

In addition to paceite, the reaction mixtures also exhibited X-ray reflections consistent with different amounts of $Ca(OAc)_2·H_2O$ or $Ca(OAc)_2·H_2O·AcOH$. The observation that both of these phases participate in the solid-state formation of paceite was verified by real-time monitoring of the reaction of $Cu(OAc)_2·H_2O$ with $Ca(OH)_2$ in an atmosphere containing vapors of water and AcOH. An analogous measurement was not possible for $CaCO_3$ as the calcium source due to formation of the gaseous CO_2 in the reaction. A detailed description of the experimental setup and its use in monitoring cocrystal formation have been recently published.[30,42]

Real-time in situ X-ray diffraction monitoring of changes in a mixture of equimolar amounts of $Ca(OH)_2$ and $Cu(OAc)_2·H_2O$ upon exposure to vapors of acetic acid and water revealed (Figure 6) the interconversion of at least five crystalline phases: $Ca(OH)_2$, $Cu(OAc)_2·H_2O$, paceite, calcium acetate monohydrate (CSD code CEJLIM), and $Ca(OAc)_2·H_2O·AcOH$ (CSD code COKJUH). Rietveld refinement of in situ PXRD data revealed a continuous drop in the content of $Ca(OH)_2$ and $Cu(OAc)_2·H_2O$ reactants over approximately 14 h. The first new crystalline phase observed in the reaction is the mixed hydrate and acetic acid solvate $Ca(OAc)_2·H_2O·AcOH$, which is detected already in the first experimental data sets. The crystalline monohydrate $Ca(OAc)_2·H_2O$ appears considerably later in the reaction, after approximately 3.5 h of aging, and is soon followed by the appearance of the paceite structure after approximately 5 h of aging. The initial formation of $Ca(OAc)_2·H_2O·AcOH$, followed by $Ca(OAc)_2·H_2O$, is consistent with previous general observations on mechanochemical reactions of oxides with carboxylic acids, which reveal the initial formation of the more solvated intermediate phases.

Rietveld analysis suggests that the disappearance of $Ca(OH)_2$ takes place faster than that of $Cu(OAc)_2·H_2O$. While quantitative analysis is hindered by significant potential for preferred orientation and crystal size effects in such a nonmixed reaction system, these observations may be explained by multiple possible reaction pathways available for calcium hydroxide, forming three different calcium-containing products, in contrast to copper(II) acetate converting only to paceite.

Cadmium Analogue of Paceite. We next explored the potential to use analogous reactivity to synthesize the previously reported cadmium analogue of paceite.[20] Indeed, the two-step mechanochemical reactions involving milling of $Ca(OH)_2$ or $CaCO_3$ in the presence of a small excess of acetic acid, followed by milling of resulting $Ca(OAc)_2·H_2O$ with commercially available $Cd(OAc)_2·2H_2O$, led to the quantitative formation of the targeted $CaCd(OAc)_4·6H_2O$ paceite analogue (Figure 7). Formation of $CaCd(OAc)_4·6H_2O$ was verified by PXRD pattern analysis, which revealed a product isostructural to paceite. As observed in the case of synthetic paceite, its cadmium analogue could also be obtained by a one-pot mechanochemical procedure starting from either $CaCO_3$ or $Ca(OH)_2$ in the presence of commercial $Cd(OAc)_2·2H_2O$, acetic acid, and a small amount of water. Again, the formation of $CaCd(OAc)_4·6H_2O$ was confirmed by PXRD analysis (Figure 7), as well as TGA (see the Supporting Information). In this case also, the formation of the same product by both

DOI: 10.1021/acsomega.9b00295
ACS Omega 2019, 4, 5486−5495

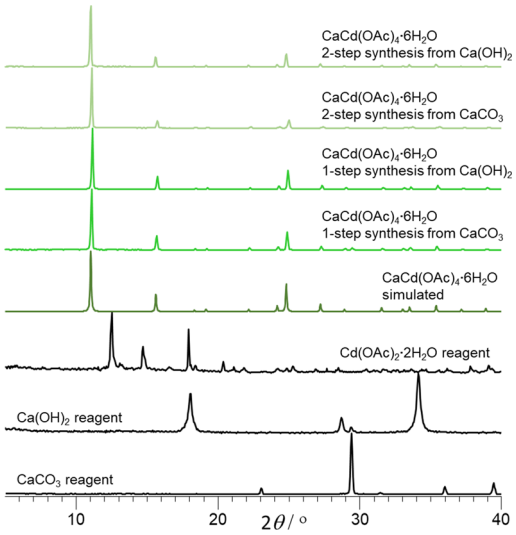

Figure 7. Comparison of PXRD patterns for $CaCd(OAc)_4{\cdot}6H_2O$ prepared from $Ca(OH)_2$ or $CaCO_3$ in a one- or two-step mechanochemical procedure to corresponding patterns of starting materials and simulated patterns of targeted products.

one- and two-step mechanochemical routes was confirmed by FTIR-ATR spectroscopy (see the Supporting Information).

As the crystallographic data for $CaCd(OAc)_4{\cdot}6H_2O$ have previously not been reported, we also conducted a single crystal X-ray diffraction study of the structure of this mixed-metal coordination polymer (Table 1). Single crystals for $CaCd(OAc)_4{\cdot}6H_2O$ were obtained through an accelerated aging process from a deliquescent mixture of equimolar amounts of $Ca(OH)_2$, $Cd(OAc)_2{\cdot}2H_2O$, and a small excess (10%) of acetic acid that was aged over 2 days at 45 °C and 100% RH.

Table 1. Crystallographic and General Data for $CaCd(OAc)_2{\cdot}6H_2O$

formula	$C_4H_{12}Ca_{0.5}Cd_{0.5}O_7$
M_r	248.4
T (K)	298(2)
crystal system	tetragonal
space group	$I4/m$
a (Å)	11.3440(4)
c (Å)	16.0488(6)
V (Å^3)	2065.3(2)
Z	8
ρ_{calc} (g/cm^3)	1.598
μ (mm^{-1})	1.362
$F(000)$	1008
crystal size (mm^3)	0.3 × 0.15 × 0.15
λ (Å)	0.71073 (Mo Kα)
2θ range for data collection (°)	7.18−66.21
no. reflections	17744
no. independent reflections	1825
no. restraints	8
no. parameters	79
S	0.990
R1, wR2 ($I \geq 2\sigma(I)$)	0.028, 0.070
R1, wR2 (all data)	0.056, 0.087
largest difference electron density peak/hole (e Å^{-3})	0.31; −0.27

Crystal structure analysis revealed coordination polymer chains of alternating Cd^{2+} and Ca^{2+} ions propagating along the 4_1-screw axis parallel to the crystallographic c-axis (Figure 8). The chains are isostructural to those of copper(II)- and calcium-based chains found in paceite.

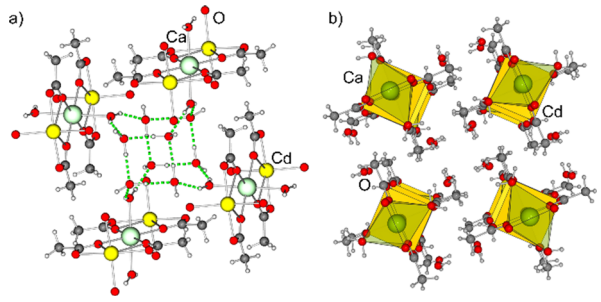

Figure 8. $CaCd(OAc)_4{\cdot}6H_2O$ crystal structure viewed along the 4_1 screw axis parallel to the crystallographic c-direction: (a) highlighting the hydrogen-bonded $(H_2O)_{12}$ cluster situated between four bimetallic coordination polymer chains and (b) similar orientation of the structure, with metal coordination polyhedra outlined (Cd: yellow, Ca: green). For clarity, the disorder of the acetate ion is not shown.

Similar to paceite, Ca^{2+} ions adopt an octahedral coordination geometry involving four equatorial acetate ions. However, in the $CaCd(OAc)_4{\cdot}6H_2O$ structure, the oxygen atom of each acetate ion associated with a Ca^{2+} ion was found to be disordered over two sites, whose relative occupational parameters were established as 0.51 and 0.49 using least-squares refinement. The disorder gives rise to two Ca···O distances of 2.31 and 2.33 Å, respectively. As in the paceite structure, each acetate ion forms a bridge to one of the two nearest-neighbor Cd^{2+} ions in a chain (Cd···O distance 2.29 Å). The apical coordination positions on each Ca^{2+} ion are occupied by oxygen atoms of two water molecule ligands (Ca···O distances 2.34 Å). Also analogous to Cu^{2+} ions, the Cd^{2+} ions in the structure of $CaCd(OAc)_4{\cdot}6H_2O$ adopt a roughly square-planar coordination geometry (O···Cd···O angle 90.7°), established through four monodentate oxygen ligands, each coming from a different acetate ion, which is also associated with a nearest-neighbor Ca^{2+} ion.

Each of the two water ligands on a Ca^{2+} ion also acts as a hydrogen bond donor to two neighboring water molecules (O−H···O distance 2.77 Å), which are further hydrogen-bonded to their symmetry-related counterparts (O−H···O separation 2.78 Å) across a 4_1-screw axis to form 12-membered cages based on O−H···O hydrogen bonds.

Enthalpies of Formation of Paceite Structures and Thermodynamic Driving Force for the Mechanochemical and Aging Formation of Paceite Structures from $CaCO_3$. In order to achieve deeper insight into the formation of paceite and its cadmium analogue from calcium carbonate, we evaluated the enthalpies of formation (ΔH_f) for both $CaCu(OAc)_4{\cdot}6H_2O$ and $CaCd(OAc)_4{\cdot}6H_2O$ using acid dissolution calorimetry[43] in 5 N aqueous hydrochloric acid as the solvent. For this purpose, dissolution enthalpies for both $CaCu(OAc)_4{\cdot}6H_2O$ and $CaCd(OAc)_4{\cdot}6H_2O$, as well as for $Cu(OAc)_2{\cdot}H_2O$, $Cd(OAc)_2{\cdot}2H_2O$, calcium acetate hydrate, $Ca(OAc)_2{\cdot}H_2O{\cdot}AcOH$, and $CaCO_3$, were experimentally determined at 25 °C. The details of experiments and collected thermodynamic data are provided in the Supporting

DOI: 10.1021/acsomega.9b00295
ACS Omega 2019, 4, 5486−5495

Table 2. Thermodynamic Data Obtained and Calculated from Acid Solution Calorimetry in 5 N HCl

compound	ΔH_s (kJ/mol)	ΔH_f (kJ/mol) from carbonate	ΔH_f (kJ/mol) from acetate
$CuCa(CH_3COO)_4{\cdot}6H_2O_{(s)}$ (synthetic paceite)	2.77 ± 0.13 (4)	−27.14 ± 0.30[a]	−31.45 ± 0.25[b]
$CdCa(CH_3COO)_4{\cdot}6H_2O_{(s)}$	−24.69 ± 0.25 (5)	−16.14 ± 0.36[c]	−20.46 ± 0.32[d]
$Ca(CH_3COO)_2{\cdot}1.1H_2O_{(s)}$	−30.00 ± 0.15 (6)		
$Cu(CH_3COO)_2{\cdot}H_2O_{(s)}$	2.68 ± 0.15 (13)		
$Cd(CH_3COO)_2{\cdot}2H_2O_{(s)}$	−14.14 ± 0.13 (4)		
$Ca(CH_3COO)_2{\cdot}H_2O{\cdot}CH_3COOH_{(s)}$	−9.24 ± 0.04 (3)		
$(Cu(CH_3COO)_2{\cdot}H_2O + Ca(CH_3COO)_2{\cdot}1.1H_2O)$ (mechanical mixture)	−27.08 ± 0.89 (2)		
$CaCO_{3(s)}$	−25.23 ± 0.22 (29)		
$CH_3COOH_{(l)}$	−0.21 ± 0.01[e]		
$H_2O_{(l)}$	−0.35[f]		

[a]For reaction 4. [b]For reaction 5. [c]For reaction 6. [d]For reaction 7. [e]Ref 44. [f]Calculated from dilution enthalpy of HCl.[45] The error is two standard deviations of the mean; the values in brackets are the numbers of experiments performed.

Information, and a summary of the data is given in Table 2. Together with measured and literature values for the dissolution enthalpies of glacial acetic acid and water, these measurements enabled the evaluation of ΔH_f for $CaCu(OAc)_4{\cdot}6H_2O$ and $CaCd(OAc)_4{\cdot}6H_2O$ from reacting the corresponding transition metal acetates either with $CaCO_3$ and acetic acid or with hydrated calcium acetate, following reactions 4−7. The sample of hydrated calcium acetate used in calorimetric measurements was found to contain a slight excess of water, corresponding to the overall formula of $Ca(OAc)_2{\cdot}1.1H_2O$, which was then used instead of the ideal composition $Ca(OAc)_2{\cdot}H_2O$ for thermodynamic calculations of reactions 5 and 7.

$$Cu(OAc)_2{\cdot}H_2O_{(s)} + CaCO_{3(s)} + 2AcOH_{(l)} + 4H_2O_{(l)} \rightarrow CuCa(OAc)_4{\cdot}6H_2O_{(s)} + CO_{2(g)} \quad (4)$$

$$Cu(OAc)_2{\cdot}H_2O_{(s)} + Ca(OAc)_2{\cdot}1.1H_2O_{(s)} + 3.9H_2O_{(l)} \rightarrow CuCa(OAc)_4{\cdot}6H_2O_{(s)} \quad (5)$$

$$Cd(OAc)_2{\cdot}2H_2O_{(s)} + CaCO_{3(s)} + 2AcOH_{(l)} + 3H_2O_{(l)} \rightarrow CdCa(OAc)_4{\cdot}6H_2O_{(s)} + CO_{2(g)} \quad (6)$$

$$Cd(OAc)_2{\cdot}2H_2O_{(s)} + Ca(OAc)_2{\cdot}1.1H_2O_{(s)} + 2.9H_2O_{(l)} \rightarrow CdCa(OAc)_4{\cdot}6H_2O_{(s)} \quad (7)$$

The measurement of enthalpies of dissolution also enabled the calculation of ΔH_f for $CaCu(OAc)_4{\cdot}6H_2O$ and $CaCd(OAc)_4{\cdot}6H_2O$ from hydrated calcium acetate, in a process corresponding to the second step of the herein reported two-step mechanochemical synthesis starting from either $CaCO_3$ or $Ca(OH)_2$. In this case also, the formation of copper(II)- and cadmium-based paceite structures was clearly exothermic, which agrees with the ease of forming $CaCu(OAc)_4{\cdot}6H_2O$ and $CaCd(OAc)_4{\cdot}6H_2O$ by mechanochemical milling of corresponding metal acetates. The ΔH_f values for the formation of $CaCu(OAc)_4{\cdot}6H_2O$ and $CaCd(OAc)_4{\cdot}6H_2O$ from $Ca(OAc)_2{\cdot}H_2O$ are more exothermic than values when starting from $CaCO_3$, which might be related to the high stability of the carbonate ion in the reactant.

The measured thermodynamic data also reveal that the ΔH_f for the formation of synthetic paceite is in each case more exothermic than for its cadmium-based analogue, indicating a destabilization effect introduced by the incorporation of cadmium. The other important distinction is that the reference states for the formation reactions of $CaCu(OAc)_4{\cdot}6H_2O$ and $CaCd(OAc)_4{\cdot}6H_2O$ are not identical, as well as that the crystal structures of the starting materials $Cu(OAc)_2{\cdot}H_2O$ and $Cd(OAc)_2{\cdot}2H_2O$ are different and have different water contents.

Tentatively, the difference in ΔH_f for synthetic paceite and its cadmium analogue might be attributed to the difference in the change of transition metal coordination during the reaction: in the $Cu(OAc)_2{\cdot}H_2O$ starting material, the Cu^{2+} ions are five-coordinated with oxygen-based ligands, whereas in $Cd(OAc)_2{\cdot}2H_2O$, the Cd^{2+} ions adopt a coordination number of 7.[46,47] However, in $CaCu(OAc)_4{\cdot}6H_2O$ and $CaCd(OAc)_4{\cdot}6H_2O$, the transition metal ions adopt a coordination number of 4. Consequently, cadmium ions undergo a more significant change in coordination number upon transformation into the paceite structure compared to copper(II) ions.[20] Such a difference might be a significant factor contributing to a diminished exothermic enthalpy of formation of $CaCd(OAc)_4{\cdot}6H_2O$ compared to synthetic paceite.

An energy diagram explaining the reaction steps that occur during the formation of $CaCu(OAc)_4{\cdot}6H_2O$ is given in Figure 9. It is drawn to conserve mass in all the reactions; thus, excess acetic acid and carbon dioxide appear in the final products together with the paceite. The top diagram shows the reaction steps when $CaCO_3$ is first milled with acetic acid to form $Ca(OAc)_2{\cdot}H_2O{\cdot}AcOH$, followed by formation of $Ca(OAc)_2{\cdot}1.1H_2O$, which is then followed by subsequent milling with $Cu(OAc)_2{\cdot}H_2O$ to form paceite. Formation of the first intermediate $Ca(OAc)_2{\cdot}H_2O{\cdot}AcOH$ was seen after short milling times, and the ease of this reaction is supported here by the exothermic enthalpy change (−16.62 ± 0.23 kJ/mol). The formation of $Ca(OAc)_2{\cdot}1.1H_2O$ is accompanied by an endothermic enthalpy change (20.94 ± 0.35 kJ/mol), which results in an intermediate that has higher energy than the reactants. The highly endothermic enthalpy is consistent with longer milling times required for the synthesis of calcium acetate monohydrate and with the loss of CO_2 gas or other volatile reaction components, where a large positive entropy can compensate for the positive enthalpy to make the overall reaction favorable in free energy. The last step of paceite formation from $Ca(OAc)_2{\cdot}1.1H_2O$ is accompanied by a strong exothermic enthalpy change of −31.45 ± 0.25 kJ/mol.

DOI: 10.1021/acsomega.9b00295
ACS Omega 2019, 4, 5486−5495

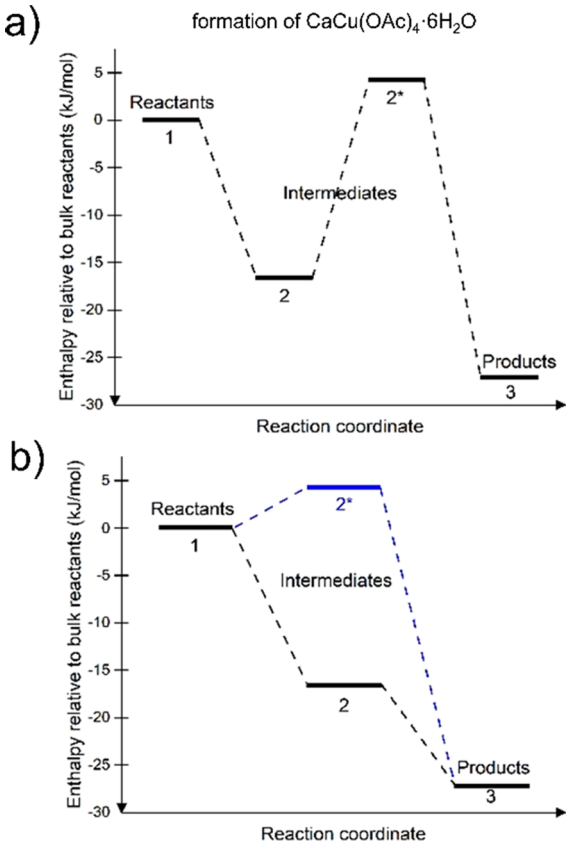

Figure 9. Energy diagram for the formation reaction of $CaCu(OAc)_2 \cdot 6H_2O$ from $CaCO_3$ and $Cu(OAc)_2 \cdot H_2O$ by considering the participation of either (a) both intermediates or (b) one intermediate. Each step corresponds to one of the following compositions: (1) $Cu(OAc)_2 \cdot H_2O_{(s)} + CaCO_{3(s)} + 3AcOH_{(l)} + 4H_2O_{(l)}$; (2) $Cu(OAc)_2 \cdot H_2O_{(s)} + Ca(OAc)_2 \cdot H_2O \cdot AcOH_{(s)} + CO_{2(g)} + 4H_2O_{(l)}$; (2*) $Cu(OAc)_2 \cdot H_2O_{(s)} + Ca(OAc)_2 \cdot 1.1H_2O_{(s)} + CO_{2(g)} + AcOH_{(l)} + 3.9H_2O_{(l)}$; (3) $CuCa(OAc)_4 \cdot 6H_2O_{(s)} + AcOH_{(l)} + CO_{2(g)}$.

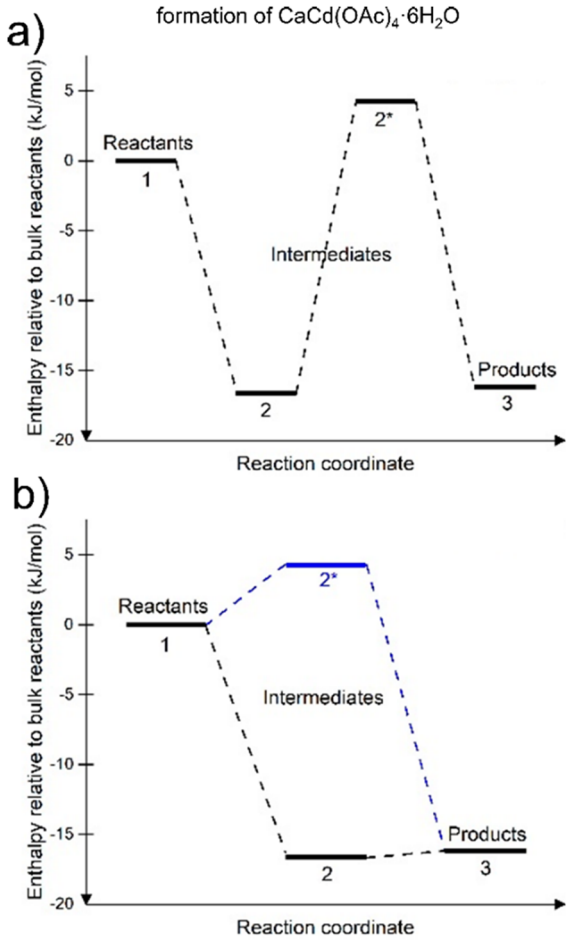

Figure 10. Energy diagram of the formation reaction of $CaCd(OAc)_2 \cdot 6H_2O$ from $CaCO_3$ and $Cd(OAc)_2 \cdot 2H_2O$ by considering the participation of either (a) both intermediates or (b) one intermediate. Each step corresponds to one of the following compositions: (1) $Cd(OAc)_2 \cdot 2H_2O_{(s)} + CaCO_{3(s)} + 3AcOH_{(l)} + 3H_2O_{(l)}$; (2) $Cd(OAc)_2 \cdot 2H_2O_{(s)} + Ca(OAc)_2 \cdot H_2O \cdot AcOH_{(s)} + CO_{2(g)} + 3H_2O_{(l)}$; (2*) $Cd(OAc)_2 \cdot 2H_2O_{(s)} + Ca(OAc)_2 \cdot 1.1H_2O_{(s)} + CO_{2(g)} + AcOH_{(l)} + 2.9H_2O_{(l)}$; (3) $CdCa(OAc)_4 \cdot 6H_2O_{(s)} + AcOH_{(l)} + CO_{2(g)}$.

Comparison of the formation of paceite directly from either of the intermediates can be seen in the bottom diagram in Figure 9. There, the black line indicates the formation through the $Ca(OAc)_2 \cdot H_2O \cdot AcOH$ intermediate, while the blue line indicates the formation through the $Ca(OAc)_2 \cdot 1.1H_2O$ intermediate. It can be seen that the $Ca(OAc)_2 \cdot 1.1H_2O$ intermediate has higher enthalpy than the bulk reactants, compared to the other intermediate that has lower enthalpy than the reactants. The formation of $Ca(OAc)_2 \cdot 1.1H_2O$ is accompanied by a small positive enthalpy change of 4.32 ± 0.27 kJ/mol. Based on these two figures, the pathway with the formation of $Ca(OAc)_2 \cdot H_2O \cdot AcOH$ appears to be the more favorable one because the intermediate lies energetically between the reactants and the products, slightly closer to the products. The reactions proceed toward lower energy and more stable forms, where the first reaction step forming the intermediate is accompanied by an enthalpy change of −16.62 ± 0.23 kJ/mol and the subsequent step of paceite formation is accompanied by an enthalpy change of −10.51 ± 0.20 kJ/mol.

Analogous diagrams for the cadmium analogue of paceite are given in Figure 10. The intermediates also have the same energy as previously, because their formation does not depend on the presence of copper(II) or cadmium acetate. In the bottom diagram, an interesting behavior is observed. The product has essentially the same enthalpy as the $Ca(OAc)_2 \cdot H_2O \cdot AcOH$ intermediate or perhaps slightly higher. The formation reaction of the product from $Ca(OAc)_2 \cdot H_2O \cdot AcOH$ is accompanied by an enthalpy change of 0.48 ± 0.29 kJ/mol, that is, essentially zero. Thus, while $Ca(OAc)_2 \cdot H_2O \cdot AcOH$ is indeed an intermediate in enthalpy between reactants and products in the case of $CaCu(OAc)_4 \cdot 6H_2O$, for $CaCd(OAc)_4 \cdot 6H_2O$ it appears to be essentially the same in enthalpy as the final product. The reason for this difference is not yet clear.

CONCLUSIONS

We have demonstrated the use of mechanochemistry for the rapid, simple, and materials-efficient preparation of synthetic samples of the organic mineral paceite and its cadmium analogue, $CaCd(OAc)_4 \cdot 6H_2O$. Importantly, while the synthesis of synthetic paceite from aqueous solutions containing copper(II) acetate and calcium acetate requires the use of an approximately 4-fold excess of the calcium reagent, mechanochemistry permits the synthesis of this material using only stoichiometric amounts of metal precursors. Furthermore, the use of mechanochemical techniques also permitted the use of

DOI: 10.1021/acsomega.9b00295
ACS Omega 2019, 4, 5486−5495

readily available calcium hydroxide or carbonate as a source of Ca^{2+}, which would be difficult to achieve using simple solution-based chemistry. Consequently, the described mechanochemical approaches illustrate the benefits of ball milling mechanochemistry in improving the control over product stoichiometry in the synthesis of coordination polymers based on two different types of metal centers and in expanding the scope of starting materials in such syntheses to poorly soluble solids. At the same time, these syntheses of synthetic paceite illustrate a poorly explored, but fast, simple, and efficient route for making synthetic samples of organic minerals. This is expected to be of high value for studies of very rare mineral species, such as hoganite, paceite, and other organic minerals. The exploration of mechanochemical reactivity also led to hints at how analogous reactions could take place in a non-agitated system by aging of reactant mixtures at high humidity and mild temperature. Such accelerated aging experiments, which mimic mineral weathering processes in a geological environment, provide a potential route for the formation of organic minerals. Importantly, thermodynamic studies based on acid dissolution calorimetry confirm that the mechanochemical syntheses of synthetic paceite and analogous aging reactions, involving known mineral species $Cu(OAc)_2{\cdot}H_2O$ (hoganite) and $CaCO_3$ (calcite), are highly exothermic. It is expected that the exothermic nature of such transformations provides sufficient driving force for the formation of paceite in a natural environment. We are currently investigating the use of mechanochemistry for the synthesis of synthetic samples of other known organic minerals.

■ ASSOCIATED CONTENT

Supporting Information

The Supporting Information is available free of charge on the ACS Publications website at DOI: 10.1021/acsomega.9b00295.

Brief description of synthetic procedures, results of thermal analysis, infrared spectroscopy, and calorimetric measurements and data relevant for thermodynamic cycle calculations (PDF)

Crystallographic data for $CaCd(OAc)_4{\cdot}6H_2O$ (CIF)

■ AUTHOR INFORMATION

Corresponding Authors

*E-mail: anavrotsky@ucdavis.edu (A.N.).
*E-mail: tomislav.friscic@mcgill.ca (T.F.).

ORCID

Hatem M. Titi: 0000-0002-0654-1292
Alexandra Navrotsky: 0000-0002-3260-0364
Tomislav Friščić: 0000-0002-3921-7915

Author Contributions

†S.L. and I.H. contributed equally. The manuscript was written through contributions of all authors. All authors have given approval to the final version of the manuscript.

Funding

NSERC Discovery Grant (RGPIN-2017-06467); E. W. R. Steacie Memorial Fellowship (SMFSU 507347−17); U.S. Department of Energy, Grant DE-SC0016573.

Notes

The authors declare no competing financial interest.

■ ACKNOWLEDGMENTS

We acknowledge the financial support of the NSERC Discovery Grant (RGPIN-2017-06467) and E. W. R. Steacie Memorial Fellowship (SMFSU 507347-17). Support for calorimetry was provided by the U.S. Department of Energy Grant DE-SC0016573.

■ ABBREVIATION

OAc^- acetate ion

■ REFERENCES

(1) Echigo, T.; Kimata, M. Crystal chemistry and genesis of organic minerals: a review of oxalate and polycyclic aromatic hydrocarbon minerals. *Can. Mineral.* **2010**, *48*, 1329−1357.
(2) Huskić, I.; Friščić, T. Understanding geology through crystal engineering: coordination complexes, coordination polymers and metal-organic frameworks as minerals. *Acta Crystallogr., Sect. B: Struct. Sci., Cryst. Eng. Mater.* **2018**, *74*, 539−559.
(3) Clarke, R. M.; Williams, I. R. Moolooite, a naturally occurring hydrated copper oxalate from Western Australia. *Mineral. Mag.* **1986**, *50*, 295−298.
(4) Guastoni, A.; Nestola, F.; Gentile, P.; Zorzi, F.; Alvaro, M.; Lanza, A.; Peruzzo, L.; Schiazza, M.; Casati, N. M. Deveroite-(Ce): a new REE-oxalate from Mount Cervandone, Devero Valley, Western-Central Alps, Italy. *Mineral. Mag.* **2013**, *77*, 3019−3026.
(5) Vranova, V.; Rejsek, K.; Formanek, P. *Sci. World J.* **2013**, 524239.
(6) Giacovazzo, C.; Menchetti, S.; Scordari, F. The crystal structure of mellite. *Acta Crystallogr., Sect. B: Struct. Sci., Cryst. Eng. Mater.* **1973**, *29*, 26−31.
(7) Bridge, P. J. Guanine and uricite, two new organic minerals from Peru and Western Australia. *Mineral. Mag.* **1974**, *39*, 889−890.
(8) Pekov, I. V.; Chukanov, N. V.; Belakovskiy, D. I.; Lykova, I. S.; Yapaskurt, V. O.; Zubkova, N.V.; Shcherbakova, E. P.; Britvin, S. N. Tinnunculite, IMA 2015-021a. CNMNC Newsletter No. 29, February 2016, page 202. *Mineral. Mag.* **2016**, *80*, 199−205.
(9) Piro, O. E.; Baran, E. J. Crystal chemistry of organic minerals − salts of organic acids: the synthetic approach. *Crystallogr. Rev.* **2018**, *24*, 149−175.
(10) Hazen, R. M.; Hummer, D. R.; Hystad, G.; Downs, R. T.; Golden, J. J. Carbon mineral ecology: predicting the undiscovered minerals of carbon. *Am. Mineral.* **2016**, *101*, 889−906.
(11) https://mineralchallenge.net/ Webpage accesed: Jan 21st 2019
(12) Hummer, D. R.; Noll, B. C.; Hazen, R. M.; Downs, R. T. Crystal structure of abelsonite, the only known crystalline geoporphyrin. *Am. Mineral.* **2017**, *102*, 1129−1132.
(13) Huskić, I.; Pekov, I. V.; Krivovichev, S. V.; Friščić, T. Minerals with metal-organic framework structures. *Sci. Adv.* **2016**, *2*, No. e1600621.
(14) Piro, O. E.; Echeverría, G. A.; González-Baró, A. C.; Baran, E. J. Crystal and molecular structure and spectroscopic behavior of isotypic synthetic analogs of the oxalate minerals stepanovite and zhemchuzhnikovite. *Phys. Chem. Miner.* **2016**, *43*, 287−300.
(15) Friščić, T. Supramolecular concepts and new techniques in mechanochemistry: cocrystals, cages, rotaxanes, open metal-organic frameworks. *Chem. Soc. Rev.* **2012**, *41*, 3493−3510.
(16) Maynard-Casely, H. E.; Hodyss, R.; Cable, M. L.; Vu, T. H.; Rahm, M. A co-crystal between benzene and ethane: a potential evaporite material for Saturn's moon Titan. *IUCrJ* **2016**, *3*, 192−199.
(17) Hibbs, D.E.; Kolitsch, U.; Leverett, P.; Sharpe, J. L.; Williams, P. A. Hoganite and paceite, two new acetate minerals from the Potosi mine, Broken Hill, Australia. *Mineral. Mag.* **2002**, *66*, 459−464.
(18) Furukawa, H.; Cordova, K. E.; O'Keeffe, M.; Yaghi, O. M. The chemistry and applications of metal-organic frameworks. *Science* **2013**, *341*, 1230444.
(19) Holden, A.; Morrison, P. *Crystals and crystal growing*; MIT Press, (1982).

DOI: 10.1021/acsomega.9b00295
ACS Omega 2019, 4, 5486−5495

(20) Langs, D. A.; Hare, C. R. The crystal structure of calcium copper acetate hexahydrate and its isomorph calcium cadmium acetate hexahydrate. *Chem. Commun. (London)* **1967**, 890−891.
(21) Klop, E. A.; Duisenberg, A. J. M.; Spek, A. L. Reinvestigation of the structure of calcium copper acetate hexahydrate, $CaCu(C_2H_3O_2)_4.6H_2O$. *Acta Crystallogr., Sect. C: Struct. Chem.* **1983**, *39*, 1342−1344.
(22) El-Bali, B.; Bolte, M. Redetermination of $[CaCu(C_2H_3O_2)_4(H_2O)_2]\cdot 6H_2O$ at 173 K. *Acta Crystallogr., Sect. C: Struct. Chem.* **1999**, *55*, IUC9900015.
(23) Furukawa, H.; Müller, U.; Yaghi, O. M. "Heterogeneity within Order" in Metal−Organic Frameworks. *Angew. Chem. Int. Ed.* **2015**, *54*, 3417−3430.
(24) Wang, L. J.; Deng, H.; Furukawa, H.; Gándara, F.; Cordova, K. E.; Peri, D.; Yaghi, O. M. Synthesis and characterization of metal-organic framework-74 containing 2, 4, 6, 8, and 10 different metals. *Inorg. Chem.* **2014**, *53*, 5881−5883.
(25) Castillo-Blas, C.; de la Peña-O'Shea, V. A.; Puente-Orench, I.; de Paz, J. R.; Sáez-Puche, R.; Gutiérrez-Puebla, E.; Gándara, F.; Monge, Á. Addressed realization of multication complex arrangements in metal-organic frameworks. *Sci. Adv.* **2017**, *3*, No. e1700773.
(26) Balarew, C.; Stoilova, D. Relation between the crystal structures of some salts of the type $Me(OCOCH_3)_2\cdot nH_2O$ and their ability to form mixed crystals or double salts (Me^{2+} = Mg, Ca, Mn, Co, Ni, Cu, Zn, Cd). *J. Solid State Chem.* **1981**, *38*, 192−198.
(27) Huskić, I.; Friščić, T. Naturally occuring metal-organic frameworks. *Acta Crystallogr., Sect. A: Found. Adv.* **2015**, *71*, s57−s58.
(28) James, S. L.; Adams, C. J.; Bolm, C.; Braga, D.; Collier, P.; Friščić, T.; Grepioni, F.; Harris, K. D. M.; Hyett, G.; Jones, W.; Krebs, A.; Mack, J.; Maini, L.; Orpen, A. G.; Parkin, I. P.; Shearouse, W. C.; Steed, J. W.; Waddell, D. C. Mechanochemistry: opportunities for new and cleaner synthesis. *Chem. Soc. Rev.* **2012**, *41*, 413−447.
(29) Mottillo, C.; Friščić, T. Advances in solid-state transformations of coordination bonds: from the ball mill to the aging chamber. *Molecules* **2017**, *22*, 144.
(30) Huskić, I.; Christopherson, J.-C.; Užarević, K.; Friščić, T. *In situ* monitoring of vapour-induced assembly of pharmaceutical cocrystals using a benchtop powder X-ray diffractometer. *Chem. Commun.* **2016**, *52*, 5120−5123.
(31) Coelho, A. *TOPAS-Academic: Version 6*; Coelho Software: Brisbane, Australia July, 2016
(32) Akimbekov, Z.; Katsenis, A. D.; Nagabhushana, G. P.; Ayoub, G.; Arhangelskis, M.; Morris, A. J.; Friščić, T.; Navrotsky, A. Experimental and theoretical evaluation of the stability of true MOF polymorphs explains their mechanochemical interconversions. *J. Am. Chem. Soc.* **2017**, *139*, 7952−7957.
(33) Štrukil, V.; Fábián, L.; Reid, D. G.; Duer, M. J.; Jackson, G. J.; Eckert-Maksić, M.; Friščić, T. Towards an environmentally-friendly laboratory: dimensionality and reactivity in the mechanosynthesis of metal-organic compounds. *Chem. Commun.* **2010**, *46*, 9191−9193.
(34) Karki, S.; Friščić, T.; Jones, W. Control and interconversion of cocrystal stoichiometry in grinding: stepwise mechanism for the formation of a hydrogen-bonded cocrystal. *CrystEngComm* **2009**, *11*, 470−481.
(35) Friščić, T.; Childs, S. L.; Rizvi, S. A. A.; Jones, W. The role of solvent in mechanochemical and sonochemical cocrystal formation: a solubility-based approach for predicting cocrystallisation outcome. *CrystEngComm* **2009**, *11*, 418−426.
(36) Friščić, T.; Halasz, I.; Strobridge, F. C.; Dinnebier, R. E.; Stein, R. S.; Fábián, L.; Curfs, C. A rational approach to screen for hydrated forms of the pharmaceutical derivative magnesium naproxen using liquid-assisted grinding. *CrystEngComm* **2011**, *13*, 3125−3129.
(37) Strobridge, F. C.; Judaš, N.; Friščić, T. A stepwise mechanism and the role of water in the liquid-assisted grinding synthesis of metal-organic materials. *CrystEngComm* **2010**, *12*, 2409−2418.
(38) Beldon, P. J.; Fábián, L.; Stein, R. S.; Thirumurugan, A.; Cheetham, A. K.; Friščić, T. Rapid room-temperature synthesis of zeolitic imidazolate frameworks by using mechanochemistry. *Angew. Chem. Int. Ed.* **2010**, *49*, 9640−9643.
(39) Bolm, C.; Mocci, R.; Schumacher, C.; Turberg, M.; Puccetti, F.; Hernández, J. G. Mechanochemical activation of iron cyano complexes: a prebiotic impact scenario for the synthesis of α-amino acid derivatives. *Angew. Chem. Int. Ed.* **2018**, *57*, 2423−2426.
(40) Qi, F.; Stein, R. S.; Friščić, T. Mimicking mineral neogenesis for the clean synthesis of metal-organic materials from mineral feedstocks: coordination polymers, MOFs and metal oxide separation. *Green Chem.* **2014**, *16*, 121−132.
(41) Banfield, J. F.; Barker, W. W.; Welch, S. A.; Taunton, A. Biological impact on mineral dissolution: Application of the lichen model to understanding mineral weathering in the rhizosphere. *Proc. Natl. Acad. Sci. U. S. A.* **1999**, *96*, 3404−3411.
(42) Lisac, K.; Nemec, V.; Topić, F.; Arhangelskis, M.; Hindle, P.; Tran, R.; Huskić, I.; Morris, A. J.; Friščić, T.; Cinčić, D. Experimental and theoretical investigation of structures, stoichiometric diversity and bench stability of cocrystals with a volatile halogen bond donor. *Cryst. Growth Des.* **2018**, *18*, 2387−2396.
(43) Hughes, J. T.; Bennett, T. D.; Cheetham, A. K.; Navrotsky, A. Thermochemistry of Zeolitic Imidazolate Frameworks of Varying Porosity. *J. Am. Chem. Soc.* **2013**, *135*, 598−601.
(44) Hughes, J. T.; Navrotsky, A. Enthalpy of Formation of Zinc Acetate Dihydrate. *J. Chem. Thermodyn.* **2011**, *43*, 980−982.
(45) Parker, V. B. *Thermal Properties of Aqueous Uni-Univalent Electrolytes*; Dept. of Commerce, National Bureau of Standards: Washington, D.C., U.S., 1965.
(46) Harrison, W.; Trotter, J. Crystal and Molecular Structure of Cadmium Diacetate Dihydrate. *Dalton Trans.* **1972**, 956−960.
(47) Brown, G. M.; Chidambaram, R. Dinuclear Copper(II) Acetate Monohydrate: A Redetermination of the Structure by Neutron-Diffraction Analysis. *Acta Crystallogr. B* **1973**, *29*, 2393−2403.

DOI: 10.1021/acsomega.9b00295
ACS Omega 2019, 4, 5486−5495